Research Square

Preprints are preliminary reports that have not undergone peer review.
They should not be considered conclusive, used to inform clinical practice,
or referenced by the media as validated information.

GIS-Based PCA–MDS Soil Fertility Index (SFI) Assessment for Coastal Soil Management

Hatim Sanad

Hatim.sanad99@gmail.com

Laboratory of Process Engineering and Environment, Faculty of Science and Technology Mohammedia, University Hassan II of Casablanca, Mohammedia 28806, Morocco

Latifa Mouhir

Laboratory of Process Engineering and Environment, Faculty of Science and Technology Mohammedia, University Hassan II of Casablanca, Mohammedia 28806, Morocco

Rachid Moussadek

International Center for Agricultural Research in the Dry Areas (ICARDA), Rabat 10100, Morocco

Majda Oueld Lhaj

Research Unit on Environment and Conservation of Natural Resources, Regional Center of Rabat, National Institute of Agriculture Research (INRA), Avenue Ennasr, Rabat 10101, Morocco

khadija Manhou

Laboratory of Natural Resources and Sustainable Development, Department of Biology, Faculty of Sciences, Ibn Tofail University, Kenitra 14000, Morocco

Houria Dakak

Research Unit on Environment and Conservation of Natural Resources, Regional Center of Rabat, National Institute of Agricultural Research, AV. Ennasr, Rabat 10101, Morocco

Abdelmjid Zouahri

Research Unit on Environment and Conservation of Natural Resources, Regional Center of Rabat, National Institute of Agricultural Research, AV. Ennasr, Rabat 10101, Morocco

---

Research Article

Keywords: Coastal soils, Soil degradation, soil health, Sustainable agriculture, Decision-support systems, Mediterranean environment

Posted Date: May 25th, 2026

DOI: https://doi.org/10.21203/rs.3.rs-9748166/v1

License: This work is licensed under a Creative Commons Attribution 4.0 International License.
Read Full License

Additional Declarations: The authors declare no competing interests.

GIS-Based PCA–MDS Soil Fertility Index (SFI) Assessment for Coastal Soil Management

Hatim Sanad [1, 2,3, *], Latifa Mouhir [1], Rachid Moussadek [4], Majda Oueld Lhaj [1, 2,3], Khadija Manhou [2, 5], Houria Dakak [2] and Abdelmjid Zouahri [2]

[a] Laboratory of Process Engineering and Environment, Faculty of Science and Technology Mohammedia, University Hassan II of Casablanca, Mohammedia 28806, Morocco;

[b] Research Unit on Environment and Conservation of Natural Resources, Regional Center of Rabat, National Institute of Agricultural Research, AV. Ennasr, Rabat 10101, Morocco;

[c] Department of Agriculture University of Napoli Federico II, Piazza Carlo di Borbone 1, Portici 80055, Italy;

[d] International Center for Agricultural Research in the Dry Areas (ICARDA), Rabat 10100, Morocco;

[e] Laboratory of Natural Resources and Sustainable Development, Department of Biology, Faculty of Sciences, Ibn Tofail University, Kenitra 14000, Morocco;

[*] Corresponding author. E-mail address: hatim.sanad99@gmail.com

Abstract

Coastal agroecosystems are increasingly vulnerable to soil degradation due to intensive agricultural practices, salinity stress, and climate-driven pressures, threatening long-term food security. The main objective is to assess soil fertility status and management suitability by combining multivariate soil diagnostics with geospatial and decision-analysis tools in the Mnasra region of the Gharb Plain, Morocco. Thirty surface soil samples (0–20 cm) were collected and analyzed for key physical and chemical properties. Multivariate statistical analyses including principal component analysis (PCA) were applied to identify dominant soil factors and derive a Minimum Data Set (MDS). A Soil Fertility Index (SFI) was then constructed using PCA-based weighting and standardized scoring, and spatially interpolated using Ordinary Kriging (OK) in GIS. Results revealed substantial variability among soil parameters, particularly in clay content (ranging from sandy to silty-clay textures), organic matter, and nutrient concentrations. Pearson correlation analysis showed strong texture-driven relationships. PCA explained 49.9% of total variance in the first component, identifying texture, carbonate content, and nutrient retention as dominant fertility controls. Based on PCA loadings, a MDS was established to construct a SFI. SFI values ranged from 0.175 to 0.836, classifying soils into low (30%), moderate (23%), good (27%), and high fertility (20%) classes. Spatial interpolation using OK revealed a clear fertility gradient from low-fertility coastal sandy soils to higher-fertility inland and river-influenced zones. The PCA–MDS–SFI framework proved effective in synthesizing complex soil variability into a quantitative, spatially interpretable fertility assessment, supporting sustainable soil management in coastal Mediterranean agroecosystems.

Keywords: Coastal soils, Soil degradation, soil health, Sustainable agriculture, Decision-support systems, Mediterranean environment

1. Inroduction

Soil health is a fundamental component of agroecosystem sustainability, particularly in coastal regions where natural and anthropogenic pressures converge (Luvai and Obiero, 2026). Coastal agroecosystems are inherently vulnerable due to their proximity to seawater, shallow groundwater tables, sandy or alluvial parent materials, and intensive land use (Agbasi et al., 2025). Although coastal zones occupy less than 20% of the Earth's land surface, they host more than 30% of the global population and support a significant proportion of high-value agricultural production systems (OECD, 2021). These areas are increasingly exposed to soil degradation processes such as salinization, erosion, nutrient depletion, and structural deterioration driven by climate variability, sea-level rise, and intensified agricultural exploitation. Globally, more than 20% of irrigated lands are affected by salinity, with coastal regions representing critical hotspots of degradation (Demo et al., 2025). In Mediterranean environments, these risks are further amplified by irregular rainfall, high evapotranspiration, and fragile sandy and silty soils, which reduce buffering capacity and increase susceptibility to compaction and nutrient loss. In North African coastal plains, including Morocco's Atlantic margin, groundwater overexploitation and seawater intrusion exacerbate these processes, leading to progressive deterioration of soil conditions and agricultural productivity (Hakimi et al., 2025; Sanad et al., 2025b).

Although often used interchangeably, the concepts of soil health, soil quality, and soil fertility represent distinct but complementary dimensions of soil functioning. Soil health refers to the overall capacity of soil to function as a living system that sustains biological productivity and environmental quality. Soil quality describes the soil's ability to perform specific functions within managed ecosystems, typically assessed through measurable physical and chemical indicators. Soil fertility represents a more specific component, focusing on the soil's capacity to supply essential nutrients to plants in adequate quantities. In this context, soil fertility constitutes a functional subset of soil quality, while soil quality contributes to the broader concept of soil health.

Soil is a non-renewable resource at human timescales and constitutes the primary medium for food production, supporting more than 95% of global food systems (FAO, 2017). Healthy soils regulate water availability, provide essential nutrients, sustain biological activity, and ensure structural support for plant growth (Imran and Ortas, 2025). However, global soil degradation has already reduced crop productivity by 10–20%, posing a significant threat to

food security for a population projected to reach 9.7 billion by 2050 (IPBES, 2018). In Morocco, agriculture contributes approximately 15% of national GDP and employs nearly 40% of the workforce, highlighting the strategic importance of soil resources for national food security (de Souza et al., 2025). Coastal plains such as the Gharb represent key agricultural zones supporting cereals, vegetables, and export-oriented horticulture (Sanad et al., 2025a). Maintaining productivity in these systems requires continuous monitoring of soil conditions and adaptive management strategies capable of addressing spatial heterogeneity and degradation risks.

Agricultural intensification has become a major driver of soil degradation when not properly managed (Manhou et al., 2025a; Oueld Lhaj et al., 2025). Practices such as intensive tillage, excessive fertilization, monocropping, and inappropriate irrigation disrupt soil structure, accelerate organic matter loss, and alter nutrient dynamics (Kim and Park, 2024). Globally, approximately 33% of soils are moderately to highly degraded, with salinization, compaction, and nutrient imbalance among the most widespread processes (Shokri et al., 2025). In coastal environments, these pressures are compounded by seawater intrusion, intensified by groundwater abstraction and sea-level rise (Hagage et al., 2024). This process increases soil salinity and sodicity, reduces nutrient availability, and limits plant growth, ultimately leading to reduced crop productivity (Gatdula and Blanco, 2024). In Morocco, coastal aquifers in regions such as the Gharb Plain have experienced increasing salinity levels, particularly in intensively irrigated areas (Sanad et al., 2026b). Associated declines in organic matter and cation exchange capacity further highlight the need for integrated soil and water management strategies (Oueld Lhaj et al., 2024a, 2024b; Manhou et al., 2025a; Batool et al., 2026).

In response to these challenges, Morocco has implemented the Green Generation 2020–2030 strategy, aimed at enhancing agricultural productivity while ensuring environmental sustainability and climate resilience (Fakhri et al., 2025; Manhou et al., 2025b). This strategy emphasizes the importance of soil diagnostics, spatial targeting of management practices, and the integration of scientific tools into agricultural planning. The promotion of geospatial analysis, digital agriculture, and decision-support systems provides a strong institutional framework for applying advanced approaches such as soil fertility indexing to guide sustainable land management in vulnerable coastal regions.

To effectively assess soil fertility variability under such complex conditions, integrative and quantitative approaches are required. The Soil Fertility Index (SFI) has emerged as a useful

metric for synthesizing multiple soil properties into a single indicator, facilitating spatial analysis and comparison of soil conditions (Acir, 2025; Oueld Lhaj et al., 2026a). SFI approaches commonly rely on multivariate techniques such as Principal Component Analysis (PCA) to derive a Minimum Data Set (MDS), reducing redundancy while preserving essential information. Previous studies have demonstrated that PCA-based indices provide meaningful insights into soil functioning and are closely associated with agricultural performance (Ibrahim et al., 2025; Shokr et al., 2025). However, the application of such integrated approaches in coastal Mediterranean agroecosystems remains limited. This study hypothesizes that a PCA-based SFI approach can effectively capture soil fertility variability and support site-specific soil management in heterogeneous coastal environments. The novelty of this research lies in the integration of multivariate statistical analysis, MDS-based index construction, and GIS-based spatial modeling to provide a coherent and spatially explicit assessment framework.

The primary aim of this study is to develop an integrated, spatially explicit framework for site-specific soil management in the Mnasra region of the Gharb Plain by combining soil physico-chemical assessment and SFI modeling. Specifically, the objectives are to:

(i) Characterize the spatial variability of soil physical and chemical properties in the coastal agricultural soils of the Mnasra region;
(ii) Identify the dominant soil factors controlling fertility using multivariate statistical analyses;
(iii) Construct a PCA-based SFI and classify soil fertility levels;
(iv) Provide a scientifically grounded decision-support tool to guide sustainable soil management and support national strategies for food security and land conservation.

2. Materials and Methods

2.1. Geographical Setting of the Study Area

The study was conducted in the Mnasra agricultural region, a coastal agroecosystem located within the Gharb Plain of northwestern Morocco. Although the Gharb Plain extends over approximately 488 km² extends from Kenitra city in the south to the Sebou River toward the north, bordered eastward by Sidi Allal Tazi and reaching the Merja Zerga lagoon near Moulay Bouselham. The western boundary is defined by the Atlantic Ocean, which exerts a strong influence on local climatic and pedological conditions. The effective investigation area considered in this study corresponded specifically to the Mnasra agricultural zone, covering approximately 30 km² **(Figure 1)**.

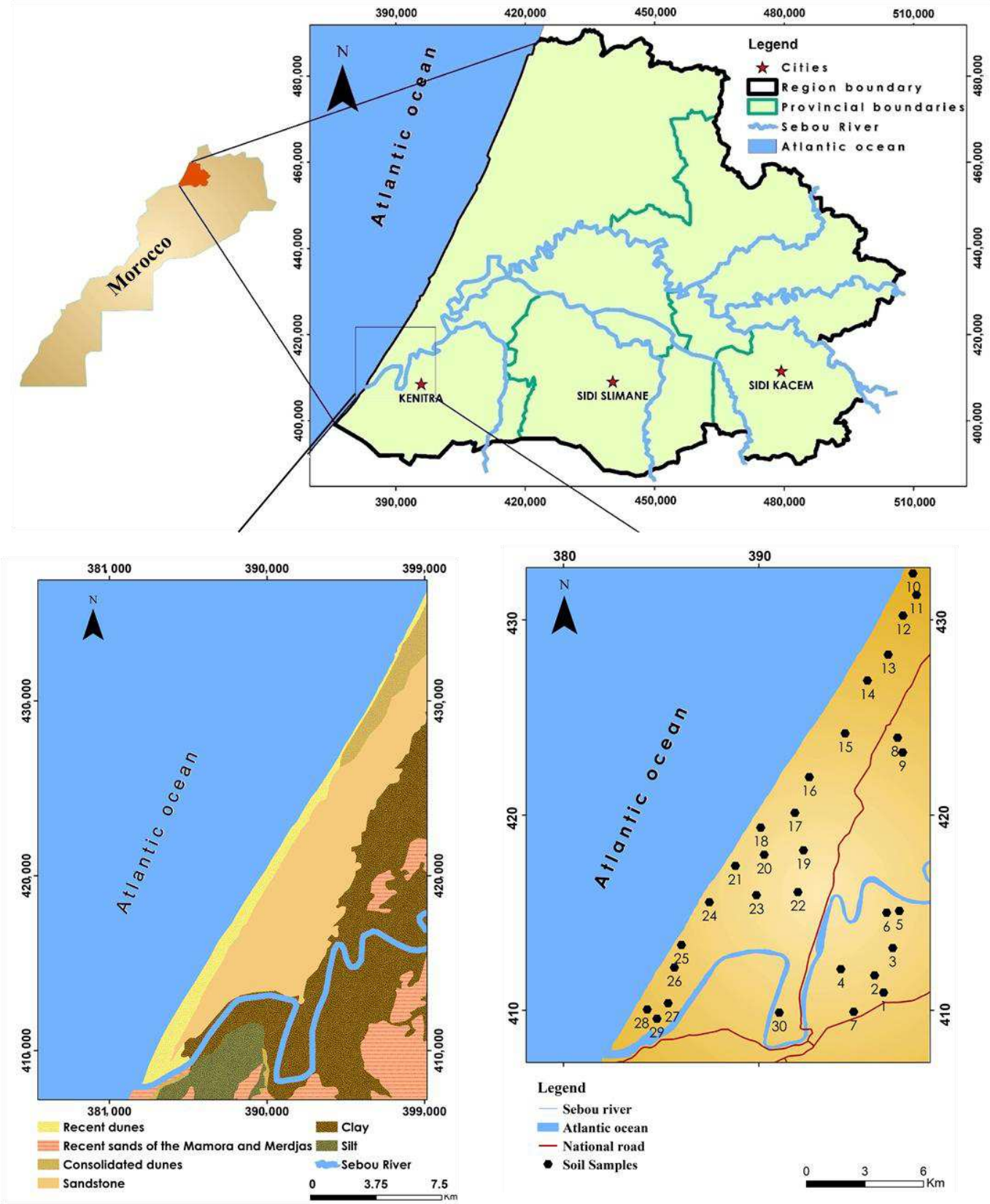


Figure 1. Map showing the location of soil samples.

Within this area, thirty georeferenced soil sampling sites were strategically distributed to capture the dominant spatial variability associated with soil texture, land use, and geomorphological conditions.

Climatically, the region is characterized by a Mediterranean regime with pronounced oceanic influence. Mean annual precipitation is approximately 550 mm, with rainfall mainly concentrated between October and April, and peak precipitation occurring during the winter months. Mean air temperatures range from approximately 12 °C in winter to 23 °C in summer. Potential evapotranspiration exceeds 150 mm during the dry season (June–September), while remaining below 80 mm during the winter period, resulting in seasonal soil moisture variability.

From a pedological perspective, the coastal strip is predominantly covered by sandy soils, representing nearly 15% of the regional surface area, while inland zones are characterized by sandy-clay and silty-clay textures. These soil characteristics, combined with intensive agricultural practices, strongly influence soil fertility dynamics across the region.

2.2. Soil Sampling Strategy and laboratory analysis

Soil sampling was conducted at thirty georeferenced sites distributed across the study area to capture the spatial heterogeneity of soil conditions. The sampling density was designed to provide representative coverage of the principal soil and agricultural variability patterns within the study area and to support multivariate statistical and spatial analyses at the regional scale of investigation. At each site, a composite soil sample was collected from the topsoil layer (0–20 cm) using a hand auger, corresponding to the active root zone of most cultivated crops. Sampling locations were selected based on inter-site distance, soil morphology, and land-use characteristics to ensure representative coverage of dominant soil types and agricultural systems.

For each sampling point, geographical coordinates, elevation, topography, and land-use information were recorded. Soil samples were placed in clean polyethylene bags and transported to the laboratory. After air-drying at ambient temperature, samples were gently crushed, cleared of visible plant residues and stones, and sieved through a 2 mm mesh to obtain a homogeneous fine-earth fraction suitable for laboratory analyses. A comprehensive suite of soil physico-chemical properties was performed to evaluate soil fertility and chemical constraints using standard laboratory procedures presented in **Table 1**.

Table 1. Soil physico-chemical parameters, analytical methods, and instruments.

Parameter	Method/Instruments	Reference
Particle size (Sand, Silt, Clay)	Hydrometer method	(Bouyoucos, 1962)
Soil moisture (%)	Gravimetric (105 °C, 24 h)	(Allen, 1989)
Bulk density (BD)	Core method	(FAO, 2023)
Porosity	Calculated from BD and PD	(FAO, 2023)
pH	Potentiometric using pH meter (Mettler Toledo Seven Easy-728 Metrohm)	(Rowell, 2014)
Electrical conductivity (EC)	Saturated paste extract and measured using conductivity meter (Orion brand, model 162)	(Page, 1983)
$CaCO_3$ (%)	Volumetric calcimetry using Collin's calcimeter	(Piper, 1947)
Organic matter (OM)	Walkley–Black oxidation	(FAO, 2020)
CEC	NH_4OAc extraction (1N)	(Rowell, 2014)
Total nitrogen (N)	Kjeldahl digestion	(Jackson, 1958)
Available phosphorus (P)	Olsen extraction using spectrophotometry analysis (JENWAY 6405 Model)	(Olsen et al., 1954)
Exchangeable K, Na	Flame photometry (Jenway PFP7 model)	(Rowell, 2014)
Exchangeable Ca, Mg	Atomic absorption spectrometry (AAS)	(Rowell, 2014)

2.3. Geospatial Analysis

Spatial analysis of soil physico-chemical properties was conducted using the Geostatistical Analyst extension in ArcGIS version 10.8 to evaluate the spatial variability of soil properties across the study area (Sanad et al., 2024a, 2024b, 2024d). All sampling locations were georeferenced in the field using handheld GPS devices and integrated into a GIS environment to establish a spatial database linking soil attributes with their geographic coordinates.

The spatial interpolation of soil properties was performed using the Ordinary Kriging (OK) method, which estimates values at unsampled locations based on the spatial autocorrelation structure of neighboring observations (Gharnate et al., 2025b, 2025a; Ngambu et al., 2025; Sanad et al., 2026a). OK assumes that the predicted value at an unknown location is a weighted linear combination of surrounding sampled values and is expressed as:

$$\hat{\mathbf{z}}(\mathbf{x_0}) = \sum_{\mathbf{i=1}}^{\mathbf{n}} \boldsymbol{\lambda_i}\, \mathbf{z}\,(\mathbf{x_i}) \quad (1)$$

where $\hat{z}(x_0)$ represents the estimated value at an unsampled location of x_0, $z(x_i)$ denotes the measured value at a sampled location x_i and n is the number of sites surrounded by the search neighborhood used for the estimation.

Spatial dependence among soil variables was evaluated using semivariogram analysis. Experimental semivariograms were computed according to (Wang and Shao, 2013; Lark, 2000):

$$\boldsymbol{\gamma(h)} = \frac{1}{2N(h)} \sum_{i=1}^{N(h)} [Z(x_i) - Z(x_i + h)]^2 \quad (2)$$

where $\gamma(h)$ represents the semivariance value for a distance h, $N(h)$ signifies the number of pairs involved in the semivariance calculation, $Z(x_i)$ denotes the value of the attribute Z at position x_i, and $Z(x_i + h)$ is the value of the attribute Z separated by a distance h from the position x_i.

Eleven semivariogram models were tested for each soil variable, and the optimal model was selected based on cross-validation performance and spatial dependence characteristics. The evaluation criteria included Mean Error (ME), Root Mean Square Error (RMSE), Mean Standardized Error (MSE), Root Mean Square Standardized Error (RMSSE), and Average Standard Error (ASE). Models presenting ME and MSE values close to zero and RMSSE values close to one were considered the most reliable for spatial prediction (Gundogdu and Guney, 2007).

The spatial distribution map of the Soil Fertility Index (SFI) was generated using the Inverse Distance Weighting (IDW) interpolation method in ArcGIS 10.8 to visualize spatial fertility gradients across the study area.

2.4. Statistical Analyses of Soil Properties

Descriptive statistics were computed using IBM SPSS Statistics 25 to characterize soil variability. Pearson correlation and hierarchical cluster analysis were applied to evaluate interrelationships among soil variables, PCA was performed to reduce data dimensionality, identify dominant factors controlling soil variability, and support the selection of a Minimum Data Set (MDS) for SFI development (Sanad et al., 2026c). Prior to PCA, the suitability of the dataset for multivariate analysis was evaluated using the Kaiser–Meyer–Olkin (KMO) measure of sampling adequacy and Bartlett's test of sphericity. The KMO value exceeded the acceptable threshold of 0.6, indicating adequate intercorrelation among variables, while Bartlett's test was statistically significant ($p < 0.05$), confirming that the correlation matrix was not an identity matrix and that PCA was appropriate. PCA was conducted using a standardized dataset (z-score normalization) to eliminate the influence of differing measurement units. Principal components were extracted based on the Kaiser criterion (eigenvalues > 1) and further evaluated using the

cumulative variance explained. Components explaining the majority of total variance were retained for interpretation and MDS development. No rotation method was applied in this study, as the primary objective was to preserve the original loading structure for selecting representative variables with the highest contribution to each principal component. Variables with high absolute loadings (≥ 0.5) within each retained component were considered significant contributors and selected as part of the MDS, while avoiding redundancy among highly correlated variables. The selected MDS was subsequently used for SFI calculation, ensuring a reduced yet representative set of soil indicators capturing the dominant variability patterns across the study area.

2.5. SFI Development Based on PCA-Derived MDS

The SFI was developed to provide a quantitative and integrative assessment of soil fertility by synthesizing key physico-chemical properties into a single dimensionless indicator (Akbar et al., 2010; Roy and Mostafa, 2024; Xie et al., 2024). The SFI framework was based on a MDS derived from PCA, with the objective of reducing data redundancy while preserving the dominant sources of soil variability (Cao et al., 2025). The developed index is intended to provide a relative assessment of soil fertility variability rather than an absolute prediction of crop performance.

2.5.1. MDS selection

The selection of the MDS followed a structured procedure combining PCA results and correlation analysis. First, principal components with eigenvalues greater than 1 were retained. Within each selected component, variables with high absolute loadings (|loading| ≥ 0.5) were considered significant contributors to soil variability.

To avoid redundancy, when multiple variables within the same component exhibited strong intercorrelations ($r > 0.7$), only one representative variable was retained based on its highest loading value and agronomic relevance. This approach ensured that the MDS captured the most influential soil properties while minimizing duplication of information.

Based on this procedure, the final MDS included variables representing key soil functions, including texture (clay), physical condition (bulk density, soil moisture), organic status (OM), nutrient retention capacity (CEC), and nutrient availability (Av. N, Av. P), as well as chemical constraints (EC and pH). Although the number of retained variables may appear

relatively high, this reflects the multidimensional nature of soil fertility and ensures that both productive potential and limiting factors are adequately represented.

2.5.2. Indicator Scoring and Standardization

To integrate variables with different units and scales, all MDS indicators were transformed into dimensionless scores ranging from 0 to 1 (Saraswat et al., 2023). The scoring approach was based on the functional relationship between each soil property and soil fertility processes, rather than simplified assumptions.

For variables positively associated with soil fertility (e.g., clay content, soil moisture, OM, CEC, available nutrients), higher values generally enhance nutrient retention, water availability, and biological activity (Li et al., 2024). These indicators were normalized using a linear scaling function (J. Wang et al., 2025):

$$\mathbf{S_i} = \frac{\mathbf{X_i} - \mathbf{X_{min}}}{\mathbf{X_{max}} - \mathbf{X_{min}}} \quad (3)$$

Conversely, variables representing constraints to soil productivity, such as BD (compaction) and EC (salinity), were treated as limiting factors. For these indicators, increasing values negatively affect soil performance, and an inverse scaling function was applied (J. Wang et al., 2025):

$$\mathbf{S_i} = \frac{\mathbf{X_{max}} - \mathbf{X_i}}{\mathbf{X_{max}} - \mathbf{X_{min}}} \quad (4)$$

For soil pH, which exhibits an optimal range for plant growth, an optimum-based scoring function was applied to account for deviations from neutrality (J. Wang et al., 2025):

$$\mathbf{S_{pH}} = \mathbf{1} - \frac{\left|\mathbf{X_i} - \mathbf{X_{opt}}\right|}{\mathbf{max}\left(\left|\mathbf{X} - \mathbf{X_{opt}}\right|\right)} \quad (5)$$

Where "X_{opt}"=7, this approach allows a more realistic representation of soil chemical suitability.

2.5.3. Weighting Scheme and SFI Calculation

The weighting of each indicator was derived from its contribution to the overall variability of the dataset, as identified by PCA. Specifically, weights were calculated based on the absolute loading values and variance contribution of each principal component, ensuring a data-driven and objective weighting scheme. The normalized weight for each indicator was expressed as:

$$\mathbf{W_i} = \frac{|\mathbf{L_i}|}{\sum|\mathbf{L_i}|} \quad (6)$$

Where "Li" represents the loading of variable "i" within the retained principal components.

The SFI for each sampling location was then calculated using a weighted linear combination (J. Wang et al., 2025):

$$\mathbf{SFI} = \sum_{i=1}^{n} \mathbf{w_i} \times \mathbf{S_i} \quad (7)$$

Where "n" is the number of MDS indicators, "S_i" is the standardized score of indicator "i", and "w_i" is its corresponding weight. The resulting SFI values range between 0 and 1, with higher values indicating better soil fertility status.

2.5.4. Methodological Scope and Validation Considerations

The SFI developed in this study is intended as a diagnostic and spatial assessment tool to evaluate soil fertility variability based on physico-chemical properties. While the index integrates key soil functions and constraints, it was not directly validated against independent agronomic indicators such as crop yield or biomass production. This limitation reflects the scope of the study, which focuses on soil system characterization and spatial variability analysis. Nevertheless, the selected indicators are widely recognized proxies of soil fertility and are strongly linked to plant growth conditions. Future research should aim to validate the SFI against field performance data to enhance its applicability for precision agriculture and decision-support systems.

2.5.5. Classification of Soil Fertility Levels

To facilitate interpretation and spatial analysis, SFI values were classified into four fertility classes using a quartile-based approach derived from the empirical distribution of SFI values **(Table 2)**.

Table 2. SFI classification (Delsouz Khaki et al., 2017; SA Rashed, 2021).

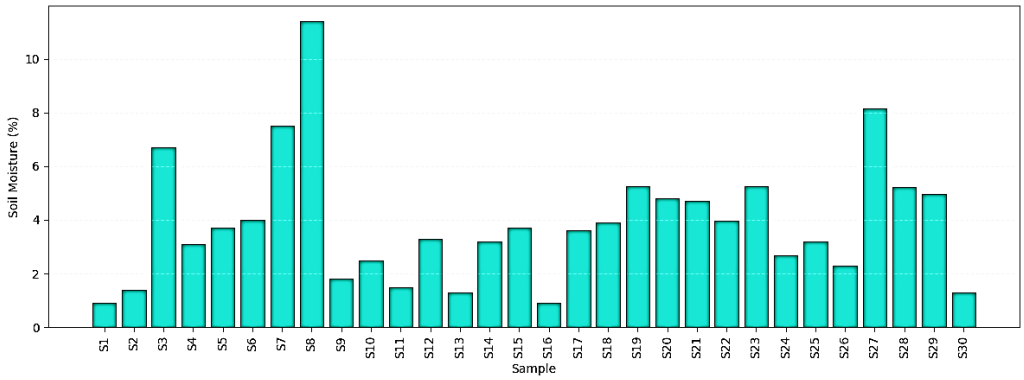
SFI Ranges	Interpretations
0.175 – 0.247	Low fertility
0.247 – 0.311	Moderate fertility
0.311 – 0.396	Good fertility
0.396 – 0.836	High fertility

3. Results

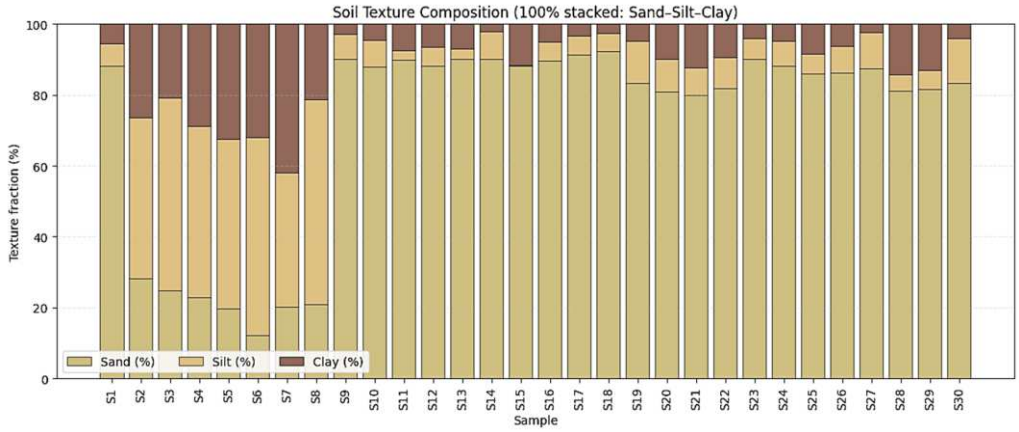
3.1. Soil physical characterization

The physical properties of soils in the Mnasra region exhibit marked spatial variability, reflecting the combined influence of coastal processes, alluvial inputs from the Sebou River, and long-term agricultural use **(Figure 2** and **Figure 3)**.

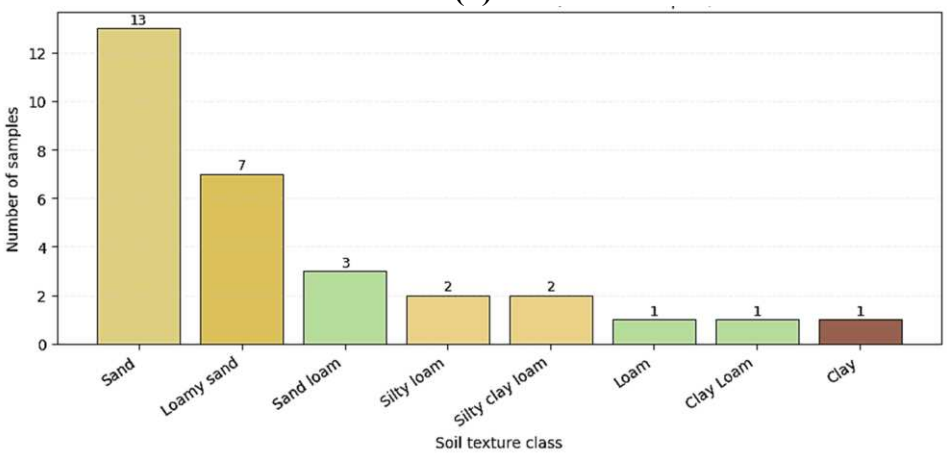
Soil moisture content ranged from 0.9% (S16) to 11.4% (S8), with a mean value of 4.01%, indicating generally dry surface conditions with localized zones of higher water retention. The highest moisture observed at S8 is consistent with finer-textured soils and proximity to fluvial influence, whereas the lowest values correspond to coarse-textured, well-drained sandy soils typical of the coastal strip. Soil texture analysis indicated a dominance of coarse materials with marked variability in USDA textural classes across the study area. Sand content ranged from 12.1% (S6) to 92.4% (S18), with a mean of 70.34%, confirming the prevalence of sandy parent materials, particularly in coastal zones. Silt varied between 0.4% (S15) and 57.7% (S8), averaging 17.40%, while clay ranged from 2.0% (S14) to 42.0% (S7), with a mean of 12.47%. Textural classes included sand and loamy sand in coastal sites, sandy loam in transitional areas, and loam to clay loam in inland and Sebou River–influenced zones. This gradient reflects contrasting sedimentary environments and establishes the physical basis for variations in water retention, compaction, and fertility processes. Bulk density (BD) ranged from 1.32 g/cm³ (S7) to 1.58 g/cm³ (S1), with a mean of 1.45 g/cm³, indicating moderate compaction overall. Lower BD values were associated with finer-textured soils, whereas higher values characterized sandy sites. Particle density showed limited variability and remained within typical mineral soil ranges. Soil porosity varied from 34.1% (S5) to 45.5% (S1), averaging 40.36%, with higher values generally observed in loosely packed sandy soils. Calcium carbonate content was relatively low, ranging from 0.0% (S9) to 4.28% (S5), with a mean of 0.77%, indicating predominantly non-calcareous to slightly calcareous soils across the region.



(a)



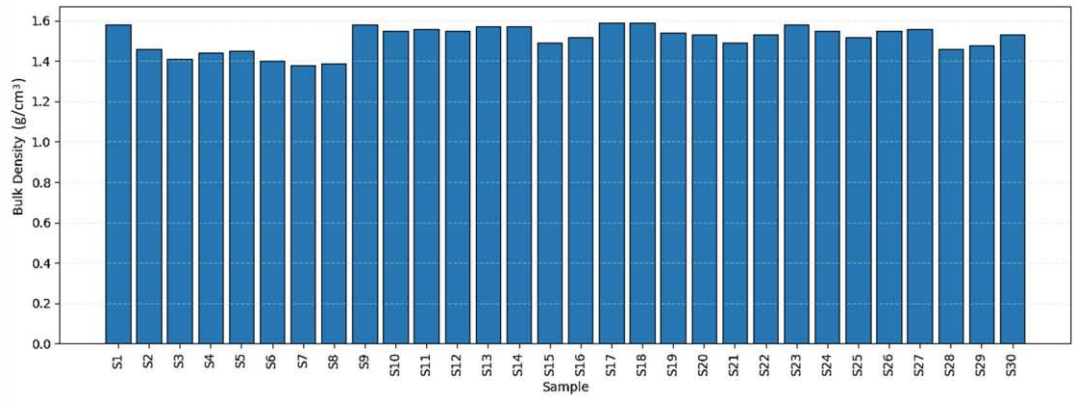
(b)



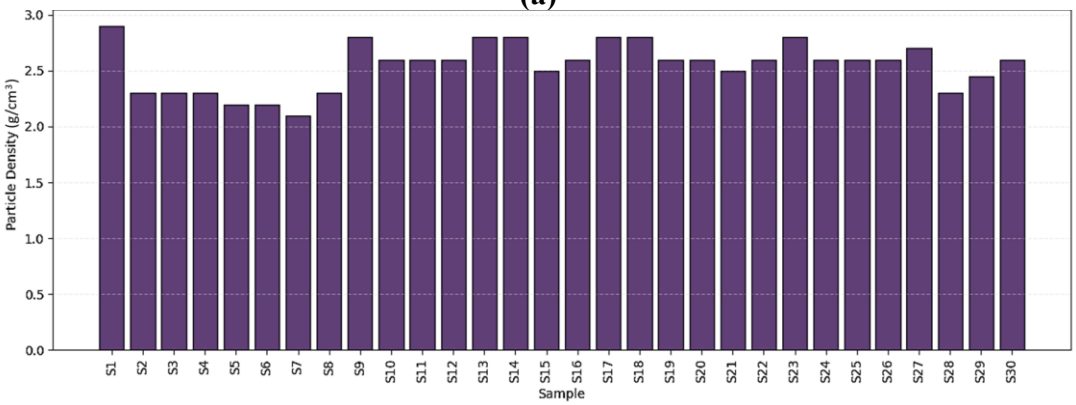
(c)

Figure 2. Graphs of (a) soil moisture content, (b) Soil texture composition and (c) soil textural classes across samples in the Mnasra region.

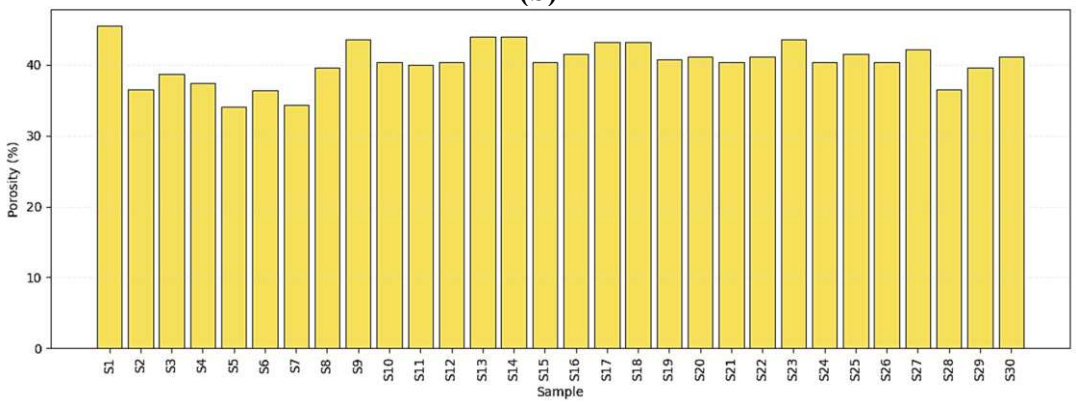
The relationships between soil structural parameters should be interpreted with caution. Although porosity is theoretically derived from bulk density and particle density, its statistical association with particle density alone may not represent a direct physical control but rather a combined effect of soil composition and structure. Therefore, the observed correlations involving porosity are better understood in the context of soil texture and bulk density, which are the primary drivers of pore space distribution in the studied soils.



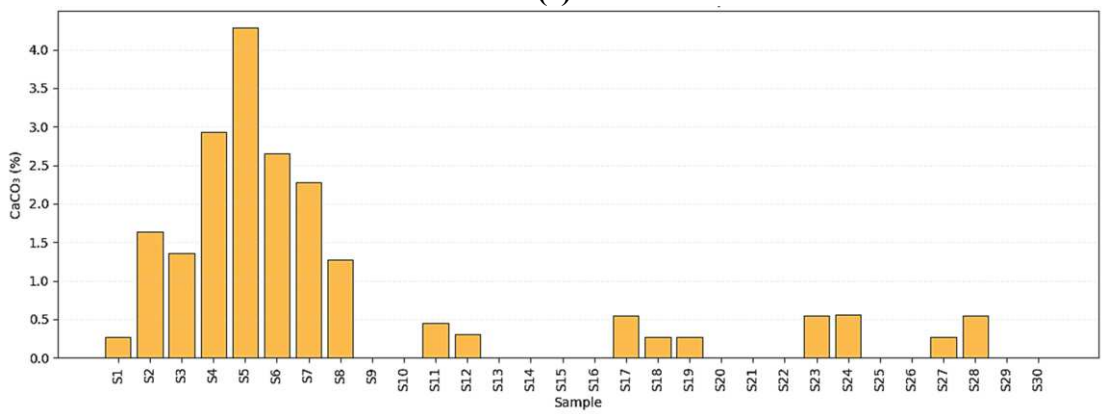
(a)



(b)



(c)



(d)

Figure 3. Distribution of (a) soil bulk density, (b) particle density, (c) soil porosity variability and (d) $CaCO_3$ content distribution in sampled agricultural soils.

3.2. Soil Chemical and nutrients variability

Soil pH values in the Mnasra agricultural soils ranged from 6.61 at sample S16 to 8.33 at sample S13, with a mean value of 7.45, indicating predominantly neutral to moderately alkaline soil conditions **(Table 3)**.

Table 3. Statistical description of soil chemical properties.

Parameters	Min	Max	Mean	Std.Dev.	CV	Skewness	Kurtosis
pH	6.61	8.33	7.46	0.38	0.05	-0.08	0.06
EC (dS/m)	0.15	3.05	0.76	0.72	0.95	1.98	3.64
OM (%)	1.61	10.08	3.4	1.67	0.49	2.37	8.03
CEC (cmol/kg)	1.34	3.11	2.09	0.52	0.24	0.44	-0.96
Av. N (mg/Kg)	65.56	193.53	107.72	38.1	0.35	0.94	-0.18
Av. P (mg/Kg)	0.82	103.47	25.81	25.56	0.99	1.63	2.41
Ex. K (mg/Kg)	65	362.5	177.5	98.59	0.55	0.62	-1.01
Na (mg/Kg)	2.83	6.54	4.78	0.62	0.13	-0.38	3.67
Ca (mg/Kg)	3	34.5	14.9	10.2	0.68	0.75	-0.91
Mg (mg/Kg)	0	9.5	3.51	2.67	0.76	0.55	-0.53

The observed variability in pH reflects differences in soil mineral composition, carbonate influence, and agricultural management practices across the study area.

EC exhibited considerable variability, ranging from 0.16 dS/m at S21 to 3.05 dS/m at S5, with an average value of 1.12 dS/m. These values indicate predominantly non-saline to moderately saline soil conditions. OM content varied between 1.62% at S9 and 10.09% at S7, with a mean value of 3.44%, reflecting heterogeneous organic matter accumulation and decomposition dynamics within the agricultural soils.

CEC ranged from 1.34 cmol/kg at S2 to 3.12 cmol/kg at S18, averaging 2.04 cmol/kg, indicating generally low to moderate nutrient retention capacity. Av. N concentrations varied from 65.56 mg/kg at S3 to 193.54 mg/kg at S27, with a mean value of 100.7 mg/kg, highlighting substantial differences in nitrogen availability among sampling sites. Av. P showed pronounced variability, ranging from 0.83 mg/kg at S1 to 103.48 mg/kg at S19, with an average value of 18.02 mg/kg, suggesting heterogeneous phosphorus availability across the agricultural landscape.

Ex. K concentrations ranged from 65.0 mg/kg at S10 to 362.5 mg/kg at S23, with a mean value of 118.6 mg/kg. Sodium concentrations varied between 2.83 mg/kg at S21 and 6.54 mg/kg at S18. Ca and Mg contents ranged from 3.0 to 34.5 mg/kg and from 0.0 to 9.5 mg/kg, respectively, reflecting variability in base cation availability and soil chemical composition among the sampled soils.

3.3. Geostatistical Modeling and Spatial Distribution of Soil Chemical Properties

The geostatistical analysis revealed marked spatial heterogeneity among the investigated soil chemical and nutrient properties across the Mnasra agricultural region. Different semivariogram models were identified as the best fit depending on the spatial behavior of each variable, including Pentaspherical, Exponential, Rational Quadratic, Spherical, K-Bessel, and Circular models (**Table 4**).

Table 4. Semivariogram parameters of the selected soil properties.

Parametres	Best-Fitted Model	Nugget	Partial Sill	Sill	Nugget/Sill	SDC	Prediction Errors				
							ME	RMSE	MSE	RMSSE	ASE
pH	Pentaspherical	14.00	0.01	14.01	1.00	Weak	0.0002	0.4121	0.0001	1.0040	0.4124
EC	Pentaspherical	0.21	0.31	0.52	0.40	Moderate	0.0001	0.6436	-0.0121	1.0279	0.6294
OM	Exponential	2.23	0.86	3.09	0.72	Moderate	-0.0491	1.8557	-0.0308	1.1149	1.6535
CEC	Exponential	0.20	0.20	0.40	0.50	Moderate	0.0064	0.4698	0.0061	0.9902	0.4774
Av. N	Rational Quadratic	134.36	1569.66	1704.02	0.08	Strong	0.0227	20.4236	-0.0074	0.8568	25.7317
Av. P	Rational Quadratic	482.63	198.86	681.49	0.71	Moderate	-0.3996	25.6871	-0.0168	1.0083	25.4855
Ex. K	Spherical	3848.17	8340.20	12188.37	0.32	Moderate	0.0218	96.2504	-0.0131	1.0418	91.4128
Na	Spherical	0.00	0.45	0.45	0.00	Strong	0.0001	0.5846	-0.0105	1.0390	0.5285
Ca	K-Bessel	52.22	85.12	137.34	0.38	Moderate	0.1509	7.6766	0.0114	0.9176	8.1934
Mg	Circular	2.63	5.11	7.74	0.34	Moderate	-0.0325	2.8651	0.0044	1.0653	2.6544

The variability in semivariogram structures reflects differences in the spatial continuity and distribution patterns of soil properties, indicating that each parameter responds differently to pedological conditions, hydrological influences, and agricultural management practices.

The nugget-to-sill ratio showed varying degrees of spatial dependence among soil variables. Strong spatial dependence was observed for Av. N and Na, with nugget-to-sill ratios of 0.08 and 0.00, respectively, suggesting that their spatial variability was mainly controlled by intrinsic environmental factors such as soil texture, parent material, and hydrological conditions. In contrast, EC, OM, CEC, Av. P, Ex. K, Ca, and Mg exhibited moderate spatial dependence, indicating that both natural factors and anthropogenic agricultural practices contributed to their spatial variability. Soil pH showed weak spatial dependence, reflecting greater local variability and reduced spatial continuity throughout the study area.

Cross-validation statistics confirmed the reliability of the selected semivariogram models and the suitability of the Ordinary Kriging interpolation approach. ME and MSE values were generally close to zero, indicating minimal estimation bias, while RMSSE values were close to one for most variables, demonstrating acceptable prediction accuracy and robustness of the spatial interpolation models.

The spatial distribution maps generated through Ordinary Kriging revealed clear spatial gradients in soil chemical properties across the study area **(Figure 4** and **Figure 5)**. Soil pH displayed a gradual transition from near-neutral conditions in the coastal strip and Sebou River–adjacent zones toward moderately alkaline conditions in the inland eastern areas, suggesting increasing carbonate influence and lower leaching intensity inland.

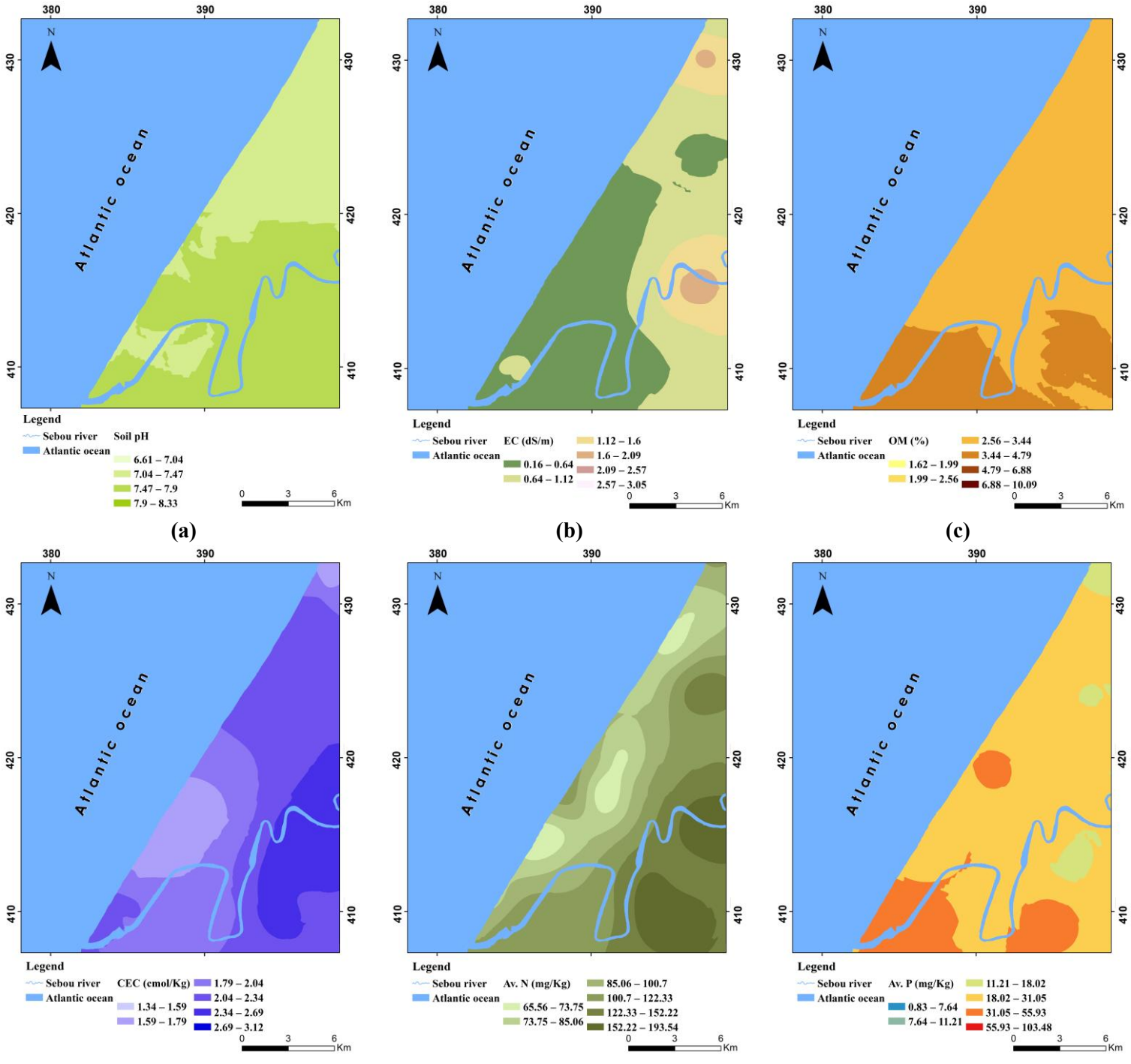


Figure 4. Spatial distribution of soil chemical parameters (a) pH, (b) EC, (c) OM, (d) CEC, (e) Av. N and (f) Av. P.

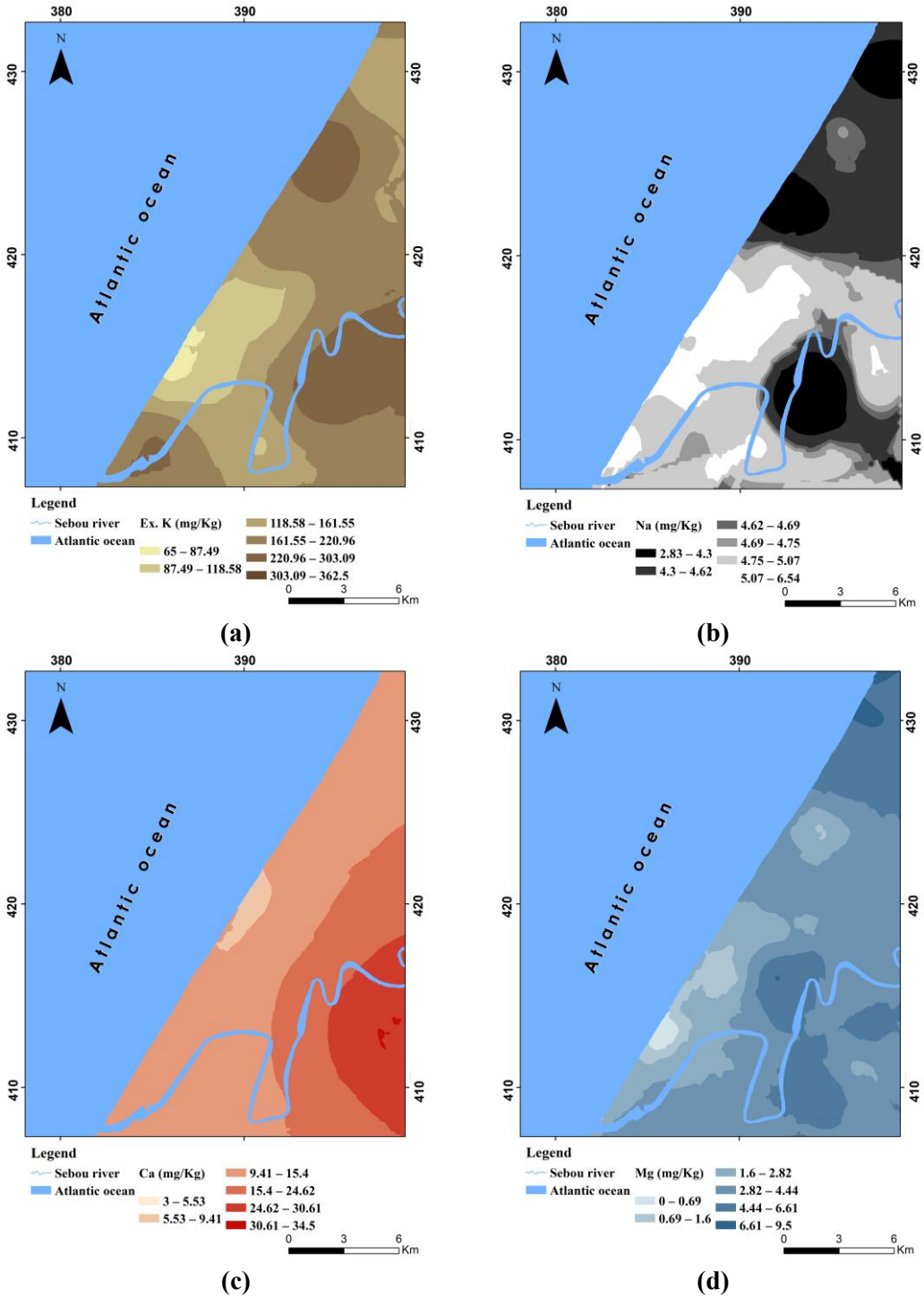


Figure 5. Spatial distribution of soil chemical parameters (a) Ex. K, (b) Na, (c) Ca and (d) Mg.

EC exhibited localized salinity enrichment zones, with higher EC values concentrated in inland and river-influenced areas, whereas lower salinity levels dominated the coastal sandy zones.

OM distribution showed greater accumulation in the southern and Sebou River–adjacent areas, while lower contents characterized the northern coastal sandy soils. This pattern reflects the combined influence of finer soil texture, improved moisture retention, and greater organic

matter stabilization in inland zones. Similarly, higher CEC values were mainly observed in inland and finer-textured soils, whereas lower nutrient retention capacity dominated the coarse-textured coastal soils.

The spatial distribution of Av. N, Ex. K, Ca, and Mg revealed comparable enrichment patterns, with higher concentrations predominantly occurring in inland and river-influenced zones. In contrast, lower nutrient concentrations characterized the coastal sandy soils, reflecting reduced retention capacity and greater susceptibility to nutrient leaching. Av. P exhibited a more heterogeneous spatial pattern with localized inland enrichment hotspots, likely associated with site-specific fertilization practices and uneven phosphorus accumulation across cultivated fields.

Overall, the spatial analysis revealed a consistent fertility gradient extending from nutrient-poor coastal sandy soils toward relatively enriched inland and Sebou River–influenced agricultural zones. These spatial patterns highlight the strong influence of soil texture, hydrological conditions, and agricultural management practices on the distribution and spatial variability of soil fertility-related properties within the Mnasra agroecosystem.

3.4. Statistical analyse

3.4.1. Correlation and HCA of Soil Physico-Chemical Properties

Pearson correlation analysis indicates that soil variability is primarily governed by texture and structural attributes **(Figure 6)**. Strong inverse relationships were observed among particle-size fractions, particularly between Sand–Silt ($r = -0.98$) and Sand–Clay ($r = -0.93$), reflecting compositional constraints. Clay and Silt were strongly positively correlated ($r = 0.83$) and exhibited strong negative relationships with BD and PD ($r \approx -0.90$), while Sand showed positive associations with both parameters ($r = 0.88–0.85$). Porosity was strongly negatively correlated with Clay ($r = -0.87$) and positively with PD ($r = 0.96$), highlighting the close coupling between texture and soil structure.

$CaCO_3$ was positively correlated with Clay, Silt, and Ca ($r = 0.83–0.85$) and negatively with Sand ($r = -0.87$), indicating preferential accumulation in fine-textured soils. pH showed moderate positive correlations with Clay, Silt, $CaCO_3$, and Ca ($r = 0.47–0.51$), while EC was moderately associated with $CaCO_3$, CEC, and Ca ($r = 0.41–0.44$). OM was positively correlated with Moisture ($r = 0.47$) and Av. P ($r = 0.51$), and negatively with BD and PD ($r \approx -0.43$), indicating greater accumulation under less compacted conditions. CEC and Av. N showed strong positive correlations with Clay, Silt, $CaCO_3$, and Ca ($r = 0.57–0.80$), confirming their dependence on fine particles and carbonate-rich matrices, whereas Av. P displayed weak correlations, reflecting a more independent spatial behavior.

It is important to note that certain strong correlations observed among particle-size fractions, particularly the negative relationships between sand and silt or clay, are primarily driven by compositional constraints, as these fractions sum to 100%. Therefore, such relationships should not be overinterpreted as independent soil processes but rather as inherent mathematical dependencies. In contrast, correlations involving structural and chemical properties, such as those linking clay content with CEC or nutrient availability, reflect meaningful pedological controls and are therefore more relevant for interpreting soil fertility dynamics.

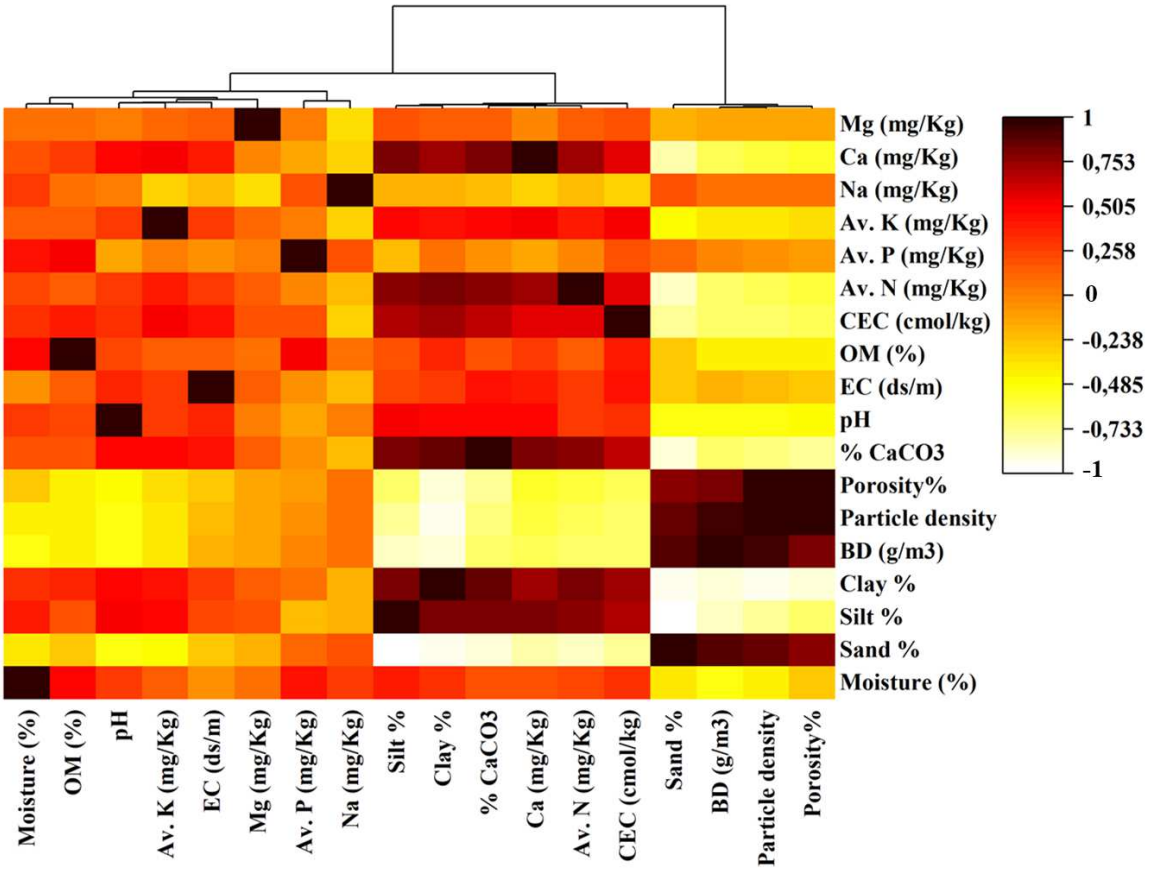


Figure 6. Heatmap of correlation analysis and HCA clustering.

The HCA dendrogram indicates that the soil variables are organized into distinct groups reflecting both textural control and nutrient-related associations. Sand is positioned close to BD, particle density, and porosity, indicating the association of coarse-textured soils with structural attributes. In contrast, clay and silt are grouped with $CaCO_3$, Ca, CEC, and Av. N, suggesting that fine-textured soils are more closely linked to carbonate content, nutrient retention capacity, and nitrogen availability. OM, Av. P, and Av. K form a separate nutrient-related cluster, reflecting their partial independence from the main texture–structure gradient and possible influence by management practices. Finally, pH, EC, Na, and Mg appear in more

distant branches, indicating more localized chemical variability rather than direct control by soil texture alone.

The combined heatmap and dendrogram representation provides an integrated visualization of the relationships among soil properties and their hierarchical organization. The clustering structure confirms that texture-related variables constitute the dominant controlling group within the dataset, while nutrient-related parameters progressively associate with this structural framework. The separation of pH, EC, and exchangeable cations into more distant branches indicates greater spatial heterogeneity and localized chemical variability compared with texture-driven parameters. This figure therefore highlights the interconnected nature of physical and chemical soil processes governing fertility distribution in the study area.

3.4.2. Principal component analysis (PCA)

The PCA revealed a clear structure in soil variability, with the first four components explaining 75.64% of the total variance **(Figure 7)**.

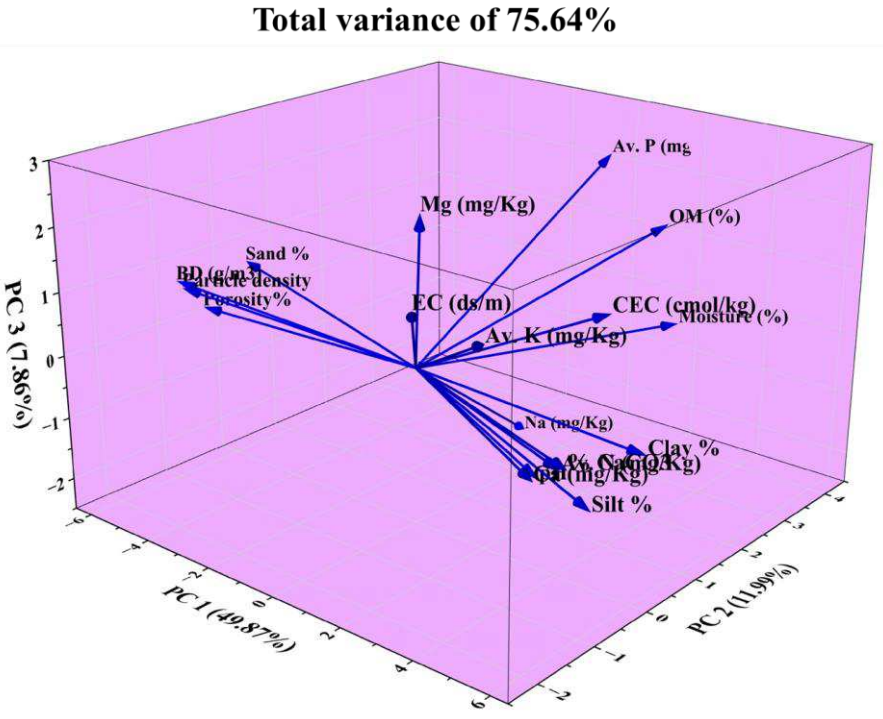


Figure 7. Graph of PCA results.

PC1 accounted for 49.87% of the variance and was strongly structured by soil texture and associated fertility indicators. Positive loadings on PC1 were dominated by Clay, Silt, $CaCO_3$, CEC, Av. N, and Ca, whereas Sand, BD, PD, and Porosity loaded negatively. This axis therefore represents a texture–fertility gradient, separating fine-textured, nutrient-retentive soils from coarse, structurally dense sandy soils. PC2, explaining 11.99% of the variance, was

primarily associated with Moisture, OM, Av. P, and Na, with all showing high positive loadings. This component reflects a soil moisture–organic enrichment gradient, distinguishing zones with higher organic matter accumulation and phosphorus availability from drier, less enriched soils. PC3 accounted for 7.86% of the variance and was characterized by strong positive loadings of EC, Mg, CEC, and Av. P, coupled with negative contributions from Na. This axis captures a chemical balance gradient, reflecting variability in salinity-related properties and secondary nutrient distribution. PC4, explaining 5.93% of the variance, was dominated by EC and pH, indicating a distinct alkalinity–salinity control that is independent of the main texture-driven variability. The scree plot confirms the dominance of PC1 and PC2, with a clear inflection after the fourth component, supporting the retention of the first four PCs for subsequent multivariate reduction and indicator selection.

The PCA biplot visually illustrates the dominant role of texture and nutrient-retention parameters in structuring soil variability across the study area. Variables associated with fertility enhancement, including clay, OM, CEC, and Av. N, clustered in the same directional space, indicating their positive interdependence. In contrast, sandy texture and bulk density were positioned oppositely, reflecting their negative influence on nutrient retention and soil functionality. The spatial dispersion of samples within the PCA space further demonstrates the heterogeneity of soil conditions between coastal sandy zones and more fertile inland areas.

3.5. MDS Selection and SFI calculation

3.5.1. MDS Selection

Based on the PCA results, a MDS was defined using the variables with the highest absolute loadings on the retained principal components (PCs with eigenvalues > 1), ensuring representation of the dominant soil processes while minimizing redundancy. From PC1 (49.87% of variance), which represents the texture–fertility gradient, Clay, CEC, and Av. N were selected due to their strong positive loadings and their central role in nutrient retention. BD was retained from the same component to capture the contrasting structural constraint associated with coarse-textured soils. From PC2 (11.99%), reflecting moisture and organic enrichment, Soil moisture and OM were selected owing to their high positive loadings and agronomic relevance. Av. P was also retained to represent nutrient availability controlled by organic and moisture dynamics. From PC3 and PC4, which describe chemical environment gradients, EC and pH were selected to capture salinity–alkalinity effects that are weakly correlated with texture but critical for soil fertility assessment. The final MDS therefore consists of Clay, BD, Moisture, OM, CEC, Av. N, Av. P, EC, and pH, which collectively represent

physical structure, nutrient retention, organic status, and chemical constraints identified by PCA.

3.5.2. SFI calculation

The SFI was calculated using the selected MDS following a standardized scoring and weighting procedure. Each indicator was first normalized to a dimensionless score ranging from 0 to 1 according to its functional relationship with soil fertility. Clay, Moisture, OM, CEC, Av. N, and Av. P were treated as positive fertility indicators, whereas BD and EC were considered limiting indicators and inversely scored. The pH was scored using an optimum-range function to account for reduced fertility under both acidic and alkaline conditions. Indicator weights were derived from PCA loading magnitudes, ensuring that variables contributing most strongly to overall variance exerted a greater influence on the final index. The SFI was computed as a weighted linear combination of the normalized MDS scores. The SFI exhibited pronounced spatial variability across the study area, reflecting the integrated effects of soil texture, structure, nutrient availability, and chemical conditions. SFI values ranged from 0.175 (S24) to 0.836 (S7) and were classified into four fertility classes including low (0.175–0.247), moderate (0.253–0.301), good (0.311–0.396), and high fertility (0.426–0.836) **(Figure 8)**.

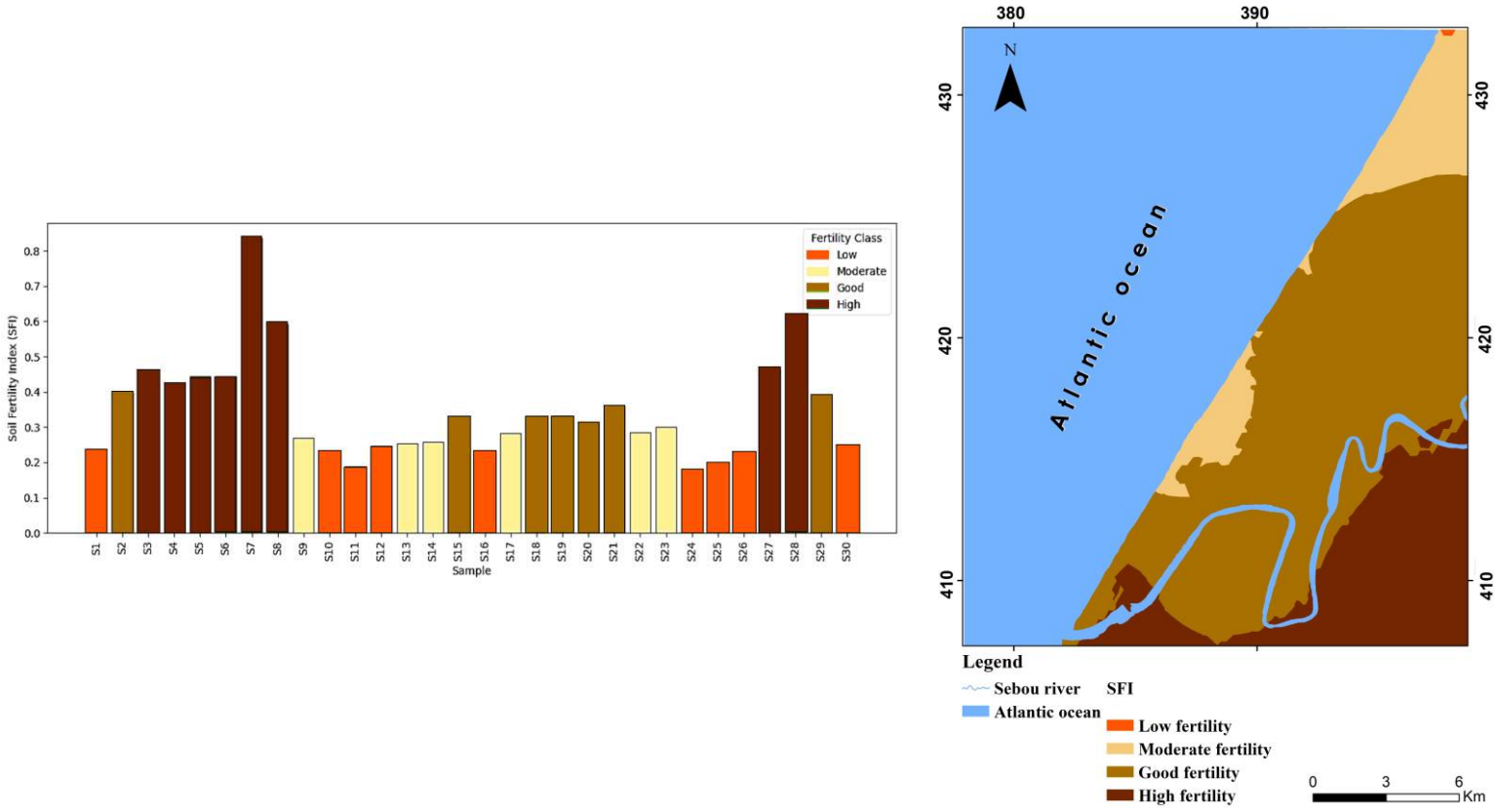


Figure 8. Variability of the SFI and fertility classes across sampling sites.

The spatial distribution of the SFI revealed marked fertility heterogeneity across the Mnasra agricultural region, following a clear gradient from low-fertility coastal soils toward more fertile inland and river-influenced zones. High-fertility areas were predominantly concentrated in the southern and inland sectors characterized by finer-textured and carbonate-influenced soils with higher organic matter, CEC, and nutrient availability, indicating favorable conditions for nutrient retention and agricultural productivity. In contrast, low-fertility classes were mainly distributed along the coastal strip and northern sandy zones, where coarse texture, higher bulk density, and reduced organic matter limited soil retention capacity and overall fertility status.

Good and moderate-fertility classes formed transitional belts between these contrasting environments, reflecting intermediate soil conditions with partial nutrient enrichment but remaining physical or chemical constraints. The spatial continuity observed in the SFI map indicates that fertility variability is strongly controlled by environmental and geomorphological gradients rather than random distribution patterns. Overall, these results highlight the influence of soil texture, hydrological conditions, and nutrient dynamics on fertility distribution and emphasize the importance of site-specific soil management strategies adapted to local soil constraints within the coastal agroecosystem.

4. Discussion

4.1. Integrated Interpretation of Soil Physico-Chemical Variability and Soil Fertility for Soil Management

The results of this study demonstrate that soil health and agricultural sustainability in the Mnasra region are primarily controlled by the strong interaction between soil texture, structural properties, nutrient retention capacity, and chemical constraints, which together shape the spatial heterogeneity of soil fertility. The pronounced dominance of texture-driven variability, revealed through correlation analysis, HCA, and PCA, confirms that clay and silt fractions play a pivotal role in regulating BD, porosity, CEC, and nutrient availability. These findings are consistent with those reported by (Sanad et al., 2024c) for the same region, who highlighted soil texture and parent material as the main drivers of soil quality variability in the Gharb Plain using a SQI approach . However, while their study primarily focused on soil quality assessment, the present work advances this understanding by explicitly linking fertility patterns to management decision zones.

The PCA results further clarified the hierarchical controls on soil fertility by separating texture–structure–fertility gradients from moisture–organic dynamics and salinity–alkalinity constraints. The strong contribution of clay, CEC, available nitrogen, and carbonate content to

the first principal component underscores the importance of fine-textured, carbonate-influenced soils in sustaining higher fertility levels (Wang et al., 2022; Oueld Lhaj et al., 2026b). Similar conclusions were reached by (Z. Wang et al., 2025) in coastal saline–alkali soils of China, where PCA-based MDS proved effective in capturing fertility variability and reducing redundancy among soil indicators . The agreement between these studies reinforces the robustness of PCA-derived MDS approaches in coastal and alluvial agricultural systems.

The SFI developed in this study revealed a clear spatial gradient, with low fertility soils predominantly located in coastal sandy zones and high fertility soils concentrated inland and near the Sebou River. This spatial pattern reflects the cumulative effect of coarse texture, higher bulk density, and limited nutrient retention in coastal areas versus finer textures, higher organic matter, and enhanced nutrient availability inland (Li et al., 2024). Comparable spatial fertility gradients were reported by (Muniammal Vediappan et al., 2025) in forest soils of Goa, where PCA-based fertility indices and geostatistical mapping identified management zones driven by soil texture and nutrient status. Although their context differs (forest ecosystems), the underlying principle of texture-controlled fertility zoning remains consistent.

From a soil health perspective, the SFI spatial patterns highlight the critical role of managing physical constraints in sandy coastal soils, where low organic matter and weak aggregation limit long-term productivity (Raheem et al., 2025; Manhou et al., 2026). Conversely, inland zones with high suitability reflect soils with greater resilience to degradation due to higher nutrient buffering capacity and improved structure (Liang et al., 2025). These findings support the growing consensus that sustainable agriculture in coastal and alluvial systems requires spatially differentiated management rather than uniform interventions (Saha and Mondal, 2025). In this context, the SFI framework functions as a decision-support bridge between soil diagnostics and practical land management, a role increasingly emphasized in recent AI- and GIS-driven agricultural studies such as (Mahalakshmi et al., 2025), where integrated data analytics enhanced the precision of agronomic decision-making and resource use efficiency.

4.2. Study Limitations and Scientific Contribution

Despite the robustness of the analytical framework, several limitations should be acknowledged when interpreting the results. First, the sampling density, although adequate for capturing regional-scale variability within the Mnasra agricultural zone, remains relatively limited for resolving fine-scale heterogeneity. While the 30 sampling sites were strategically distributed to represent dominant soil and land-use conditions, increasing the sampling density

would improve the precision of statistical relationships and enhance the accuracy of spatial interpolation. This limitation is particularly relevant for heterogeneous coastal environments, where soil properties may vary over short distances.

Second, uncertainties associated with geostatistical interpolation should be considered. Although Ordinary Kriging was applied using optimized semivariogram models and validated through cross-validation metrics, spatial predictions inherently involve estimation errors, especially in areas with sparse sampling coverage. The moderate to weak spatial dependence observed for some variables further suggests that local variability may not be fully captured, which could influence the interpretation of spatial distribution patterns.

Third, the construction of the SFI involves methodological simplifications. Although the use of a PCA-derived MDS reduces redundancy and enhances interpretability, the selection of indicators and scoring functions may not fully capture the complexity of soil–plant interactions. In particular, the use of linear and optimum-based scoring functions represents a simplified representation of soil processes, and the weighting scheme, while data-driven, does not explicitly account for dynamic biological or crop-specific responses. Additionally, the SFI was not validated against independent agronomic indicators such as crop yield or biomass production, which limits its direct applicability as a predictive tool for agricultural performance.

Notwithstanding these limitations, the present study provides several important scientific contributions. Unlike conventional soil fertility assessments that rely either on descriptive statistics or isolated indices, this research integrates multivariate statistical analysis, PCA-based MDS selection, Soil Fertility Index modeling, and GIS-based spatial analysis into a unified and reproducible framework. This integration allows for a more comprehensive understanding of soil variability by linking physical structure, chemical properties, and nutrient dynamics within a spatial context.

Moreover, the study advances existing knowledge by explicitly addressing soil fertility variability in a coastal Mediterranean agroecosystem, where the combined effects of sandy textures, hydrological gradients, and agricultural practices create complex spatial patterns. The identification of clear fertility gradients from coastal sandy soils to inland and river-influenced zones provides new insights into the spatial organization of soil resources in the Gharb Plain. In addition, the application of a PCA-driven MDS approach tailored to local soil conditions contributes to methodological refinement by demonstrating how data reduction techniques can be effectively adapted to heterogeneous agricultural systems.

Overall, while the findings confirm well-established relationships between soil texture, structure, and fertility, the novelty of this study lies in the integration of statistical, spatial, and

index-based approaches into a coherent framework that enhances the interpretation of soil variability and supports more informed soil management strategies. Future research should aim to incorporate higher sampling densities, temporal monitoring, and field-based validation to further strengthen the applicability of the proposed approach for precision agriculture and sustainable land management.

5. Conclusion

This study assessed soil fertility variability in the coastal agroecosystem of the Mnasra region by integrating soil physico-chemical analysis, multivariate statistics, and GIS-based spatial modeling. The results showed that soil fertility was strongly influenced by texture-related properties, particularly clay and silt fractions, which controlled nutrient retention, organic matter accumulation, and chemical behavior. Spatial analysis revealed a clear gradient from low-fertility sandy coastal soils toward more fertile inland and river-influenced zones characterized by higher CEC, OM, and nutrient availability.

PCA enabled the identification of the dominant factors controlling soil variability and supported the development of a MDS for SFI construction. The SFI successfully integrated multiple soil indicators into a single quantitative index and highlighted distinct fertility classes across the study area. The generated spatial maps provided a clear representation of fertility distribution and soil management constraints in this heterogeneous coastal environment.

The study also demonstrated the usefulness of combining PCA-based data reduction with geostatistical mapping for evaluating spatial soil fertility patterns in Mediterranean coastal agroecosystems. Nevertheless, some limitations remain related to sampling density, interpolation uncertainty, and the absence of validation using independent agronomic indicators such as crop yield or biomass production.

Overall, the proposed approach provides a practical framework for identifying soil fertility variability and supports site-specific soil management strategies aimed at improving agricultural sustainability in vulnerable coastal regions.

Conflicts of interest

The authors declare that they have no known competing financial interests or personal relationships that could have appeared to influence the work reported in this paper.

Acknowledgments

The authors are grateful to all collaborators who participated in field sampling, laboratory analyses, and manuscript preparation.

References

Acir, N., 2025. Predicting Soil Fertility in Semi-Arid Agroecosystems Using Interpretable Machine Learning Models: A Sustainable Approach for Data-Sparse Regions. Sustainability 17, 7547.

Agbasi, J.C., Abu, M., Pande, C.B., Uwajingba, H.C., Abba, S.I., Egbueri, J.C., 2025. Groundwater salinization in coastal regions and the control mechanisms: Insights for sustainable groundwater development and management, in: Sustainable Groundwater and Environment: Challenges and Solutions. Springer, pp. 165–191.

Akbar, M.H., Ahmed, O.H., Jamaluddin, A.S., Majid, N.M.N.Ab., Abdul-Hamid, H., Jusop, S., Hassan, A., Yusof, K.H., Abdu, A., 2010. Differences in Soil Physical and Chemical Properties of Rehabilitated and Secondary Forests. American Journal of Applied Sciences 7, 1200–1209. https://doi.org/10.3844/ajassp.2010.1200.1209

Allen, C., S.E. and Grimshaw, H.M. and Parkinson, J.A. and Quarmby, 1989. Chemical analysis of ecological materials. Blackwell Scientific Publications., Oxford.

Batool, A., Zhang, K., Abbas, F., Akhtar, A., Mao, J., 2026. A Comparative Evaluation of Soil Amendments in Mitigating Soil Salinization and Modifying Geochemical Processes in Arid Land. Agronomy 16, 222.

Bouyoucos, G.J., 1962. Hydrometer Method Improved for Making Particle Size Analyses of Soils1. Agronomy Journal 54, 464–465. https://doi.org/10.2134/agronj1962.00021962005400050028x

Cao, Y., Zhang, W., Pan, B., Dai, L., Tian, A., 2025. Selection of the minimum data set and quantitative soil quality indices for different azalea forest communities in southwestern China. Plant and Soil 511, 463–481.

de Souza, P.M., Zeghmane, A., Daihi, D., Ouedraogo, D.D., ElKindoussy, F., Gandiya, F., Rasaq, H.O., Temesgen, M., Ebrahim, M., Tinashe, M., 2025. Morocco's agrifood transformation: A regional model for sustainable agricultural development. Outlook on Agriculture 54, 373–386.

Delsouz Khaki, B., Honarjoo, N., Davatgar, N., Jalalian, A., Torabi Golsefidi, H., 2017. Assessment of two soil fertility indexes to evaluate paddy fields for rice cultivation. Sustainability 9, 1299.

Demo, A.H., Gemeda, M.K., Abdo, D.R., Guluma, T.N., Adugna, D.B., 2025. Impact of soil salinity, sodicity, and irrigation water salinity on crop production and coping mechanism in areas of dryland farming. Agrosystems, Geosciences & Environment 8, e70072.

Fakhri, R., Hassouni, Y.L., Moussadek, R., Dalaa, L., Bouanan, I., 2025. Country report for Morocco. Presented at the Legal Pathways to Sustainable Soil Management in Africa, Nomos Verlagsgesellschaft mbH & Co. KG, pp. 349–392.

FAO, 2023. Standard operating procedure for soil bulk density, cylinder method. FAO, Rome, Italy. https://doi.org/10.4060/cc7568en

FAO, 2020. Standard operating procedure for soil organic carbon. Walkley-Black method: titration and colorimetric method, 1st ed. FAO, Rome, Italy.

FAO, 2017. Cherishing the ground we walk on [WWW Document]. Newsroom. URL https://www.fao.org/newsroom/story/cherishing-the-ground-we-walk-on/en (accessed 2.2.26).

Gatdula, N., Blanco, A., 2024. Assessment of the vulnerability of coastal agriculture to seawater intrusion using remote sensing, GIS, and Multi-Criteria Decision Analysis. International Journal of Digital Earth 17, 2367733.

Gharnate, A., Cox, R., Sanad, H., Taouali, O., Oueld Lhaj, M., Mhammdi, N., 2025a. Hydrodynamic Modelling and Morphometric Assessment of Supratidal Boulder Transport on the Moroccan Atlantic Coast: A Dual-Site Analysis. Earth 6. https://doi.org/10.3390/earth6040124

Gharnate, A., Sanad, H., Oueld Lhaj, M., Mhammdi, N., 2025b. A Comprehensive Review of Polygenetic Signatures, Methodological Advances, and Implications for Coastal Boulder Deposits (CBDs) Assessment. GeoHazards 6. https://doi.org/10.3390/geohazards6040069

Gundogdu, K.S., Guney, I., 2007. Spatial analyses of groundwater levels using universal kriging. Journal of Earth System Science 116, 49–55. https://doi.org/10.1007/s12040-007-0006-6

Hagage, M., Abdulaziz, A.M., Elbeih, S.F., Hewaidy, A.G.A., 2024. Monitoring soil salinization and waterlogging in the northeastern Nile Delta linked to shallow saline groundwater and irrigation water quality. Scientific Reports 14, 27838. https://doi.org/10.1038/s41598-024-77954-x

Hakimi, S., Hessane, M.A., Bahir, M., Faraj, T.K., Carreira, P.M., 2025. Development of Transient Hydrodynamic and Hydrodispesive Models in Semi-Arid Environments. Hydrology 12, 46.

Ibrahim, H.M., Alasmary, Z., Majrashi, M.A., Harbi, M.A., Abldubise, A., Alghamdi, A.G., 2025. Application of Principal Component and Multi-Criteria Analysis to Evaluate Key Physical and Chemical Soil Indicators for Sustainable Land Use Management in Arid Rangeland Ecosystems. Land 14, 2167.

Imran, Ortas, I., 2025. Mechanism in Soil Health Improvement with Soil Microbial Actions and Its Role in Potential Agriculture. Communications in Soil Science and Plant Analysis 1–22.

IPBES, 2018. The IPBES assessment report on land degradation and restoration. https://doi.org/10.5281/zenodo.3237393

Jackson, M.L., 1958. Soil Chemical Analysis. Prentice Hall Inc.

Kim, H.N., Park, J.H., 2024. Monitoring of soil EC for the prediction of soil nutrient regime under different soil water and organic matter contents. Applied Biological Chemistry 67, 1. https://doi.org/10.1186/s13765-023-00849-4

Lark, R.M., 2000. Estimating variograms of soil properties by the method-of-moments and maximum likelihood. European Journal of Soil Science 51, 717–728. https://doi.org/10.1046/j.1365-2389.2000.00345.x

Li, P., Zhang, Y., Li, C., Chen, Z., Ying, D., Tian, S., Zhao, G., Ye, D., Cheng, C., Wu, C., 2024. Assessing the alteration of soil quality under long-term fertilization management in farmland soil: Integrating a minimum data set and developing new biological indicators. Agronomy 14, 1552.

Liang, X., Yu, S., Ju, Y., Wang, Y., Yin, D., 2025. Integrated management practices foster soil health, productivity, and agroecosystem resilience. Agronomy 15, 1816.

Luvai, A.K., Obiero, J.P., 2026. Drift Seaweed as a Multifunctional Resource for Sustainable Coastal Agroecosystems. Applied and Environmental Soil Science 2026, 4013072.

Mahalakshmi, S., Anand, A.J., Partheeban, P., 2025. Soil and crop interaction analysis for yield prediction with satellite imagery and deep learning techniques for the coastal regions. Journal of Environmental Management 380, 125095. https://doi.org/10.1016/j.jenvman.2025.125095

Manhou, K., Hmouni, D., Moussadek, R., Zouahri, A., Yachou, H., Lhaj, M.O., Sanad, H., Ghanimi, A., Dakak, H., 2026. Compost application enhances soil quality, growth, and yield of durum wheat under saline conditions. Scientific Reports. https://doi.org/10.1038/s41598-026-36306-7

Manhou, K., Moussadek, R., Dakak, H., Zouahri, A., Ghanimi, A., Sanad, H., Oueld Lhaj, M., Hmouni, D., 2025a. Effect of Irrigation with Saline Water on Germination, Physiology, Growth, and Yield of Durum Wheat Varieties on Silty Clay Soil. Agriculture 15. https://doi.org/10.3390/agriculture15222364

Manhou, K., Taghouti, M., Moussadek, R., Elyacoubi, H., Bennani, S., Zouahri, A., Ghanimi, A., Sanad, H., Oueld Lhaj, M., Hmouni, D., Dakak, H., 2025b. Performance, Agro-Morphological, and

Quality Traits of Durum Wheat (Triticum turgidum L. ssp. durum Desf.) Germplasm: A Case Study in Jemâa Shaïm, Morocco. Plants 14. https://doi.org/10.3390/plants14101508

Muniammal Vediappan, D., Godi, A., Golla, B., 2025. Geospatial Mapping of Soil Properties of Forest Types Using the k-Means Fuzzy Clustering Approach to Delineate Site-Specific Nutrient Management Zones in Goa, India. Journal of the Indian Society of Remote Sensing 53, 2057–2085. https://doi.org/10.1007/s12524-024-02082-y

Ngambu, A.A., Lemnyuy, P.Y., Ralain, B.N., SIMOU, A., Hatim, S., Njolai, M., Fuofu, H.F., Bertrand, K.F., Pierre, W., Kouankap, N.G.D., Oliver, A.N., 2025. Multivariate analysis and risk assessment of trace metal contamination in sediments of Mesue-Tonkwen, Cameroon: Implications for mineral exploration and ecosystem health. China Geology.

OECD, 2021. Adapting to a changing climate in the management of coastal zones. OECD Environment Policy Papers. https://doi.org/10.1787/b21083c5-en

Olsen, S.R., Cole, C.V., Watanabe, F.S., Dean, L.A., United States Department of Agriculture, 1954. Estimation of available phosphorus in soils by extraction with sodium bicarbonate. U.S. Dept. of Agriculture Washington, D.C., Washington, D.C.

Oueld Lhaj, M., Moussadek, R., Mouhir, L., Mdarhri Alaoui, M., Sanad, H., Iben Halima, O., Zouahri, A., 2024a. Assessing the Evolution of Stability and Maturity in Co-Composting Sheep Manure with Green Waste Using Physico-Chemical and Biological Properties and Statistical Analyses: A Case Study of Botanique Garden in Rabat, Morocco. Agronomy 14. https://doi.org/10.3390/agronomy14071573

Oueld Lhaj, M., Moussadek, R., Mouhir, L., Sanad, H., Manhou, K., Iben Halima, O., Yachou, H., Zouahri, A., Mdarhri Alaoui, M., 2025. Application of Compost as an Organic Amendment for Enhancing Soil Quality and Sweet Basil (Ocimum basilicum L.) Growth: Agronomic and Ecotoxicological Evaluation. Agronomy 15. https://doi.org/10.3390/agronomy15051045

Oueld Lhaj, M., Moussadek, R., Sanad, H., Zouahri, A., Manhou, K., Alaoui, M.M., Mouhir, L., 2026a. Compost improves soil fertility index and tomato (Lycopersicon esculentum L.) yield under drought: integrating multivariate soil–plant modeling and Monte Carlo Simulation across sandy loam and silty clay soils. Frontiers in Sustainable Food Systems Volume 10-2026. https://doi.org/10.3389/fsufs.2026.1797471

Oueld Lhaj, M., Moussadek, R., Zouahri, A., Sanad, H., Saafadi, L., Mdarhri Alaoui, M., Mouhir, L., 2024b. Sustainable Agriculture Through Agricultural Waste Management: A Comprehensive Review of Composting's Impact on Soil Health in Moroccan Agricultural Ecosystems. Agriculture 14. https://doi.org/10.3390/agriculture14122356

Oueld Lhaj, Majda, Moussadek, R., Sanad, H., Manhou, K., Oueld Lhaj, M'hamed, Mdarhri Alaoui, M., Zouahri, A., Mouhir, L., 2026b. Ecological and Microbial Processes in Green Waste Co-Composting for Pathogen Control and Evaluation of Compost Quality Index (CQI) Toward Agricultural Biosafety. Environments 13. https://doi.org/10.3390/environments13010043

Page, A.L. (Ed.), 1983. Methods of Soil Analysis: Part 2 Chemical and Microbiological Properties, in: Agronomy Monographs. American Society of Agronomy, Soil Science Society of America, Madison, WI, USA. https://doi.org/10.2134/agronmonogr9.2.2ed

Piper, C.S., 1947. Soil and Plant Analysis. International Science Publishers Inc.: New York, NY, USA,.

Raheem, A., Bankole, O.O., Danso, F., Musa, M.O., Adegbite, T.A., Simpson, V.B., 2025. Physical Management Strategies for Enhancing Soil Resilience to Climate Change: Insights From Africa. European Journal of Soil Science 76, e70030.

Rowell, D.L., 2014. Soil Science: Methods & Applications. Routledge, London. https://doi.org/10.4324/9781315844855

Roy, A., Mostafa, M., 2024. Impact assessment of tobacco cultivation on soil ecosystem using multi-evaluation techniques. Asian Journal of Environmental Research 1, 217–236.

SA Rashed, H., 2021. Assessment of Soil Fertility and Suitability for Some Crops Using Gis and Remote Sensing Techniques. Annals of Agricultural Science, Moshtohor 59, 1065–1076.

Saha, S., Mondal, P., 2025. Policy zoning for climate-resilient agriculture: a spatial assessment of agricultural sensitivity and resilience to environmental change in West Bengal, India. Environment, Development and Sustainability 1–31.

Sanad, H., Mouhir, L., Zouahri, A., Moussadek, R., El Azhari, H., Yachou, H., Ghanimi, A., Oueld Lhaj, M., Dakak, H., 2024a. Assessment of Groundwater Quality Using the Pollution Index of Groundwater (PIG), Nitrate Pollution Index (NPI), Water Quality Index (WQI), Multivariate Statistical Analysis (MSA), and GIS Approaches: A Case Study of the Mnasra Region, Gharb Plain, Morocco. Water 16, 1263. https://doi.org/10.3390/w16091263

Sanad, H., Moussadek, R., Dakak, H., Zouahri, A., Oueld Lhaj, M., Mouhir, L., 2024b. Ecological and Health Risk Assessment of Heavy Metals in Groundwater within an Agricultural Ecosystem Using GIS and Multivariate Statistical Analysis (MSA): A Case Study of the Mnasra Region, Gharb Plain, Morocco. Water 16. https://doi.org/10.3390/w16172417

Sanad, H., Moussadek, R., Mouhir, L., Lhaj, M.O., Zahidi, K., Dakak, H., Manhou, K., Zouahri, A., 2025a. Ecological and Human Health Hazards Evaluation of Toxic Metal Contamination in Agricultural Lands Using Multi-Index and Geostatistical Techniques across the Mnasra Area of Morocco's Gharb Plain Region. Journal of Hazardous Materials Advances 100724. https://doi.org/10.1016/j.hazadv.2025.100724

Sanad, H., Moussadek, R., Mouhir, L., Oueld Lhaj, M., Dakak, H., El Azhari, H., Yachou, H., Ghanimi, A., Zouahri, A., 2024c. Assessment of Soil Spatial Variability in Agricultural Ecosystems Using Multivariate Analysis, Soil Quality Index (SQI), and Geostatistical Approach: A Case Study of the Mnasra Region, Gharb Plain, Morocco. Agronomy 14. https://doi.org/10.3390/agronomy14061112

Sanad, H., Moussadek, R., Mouhir, L., Zouahri, A., Oueld Lhaj, M., Monsif, Y., Manhou, K., Dakak, H., 2026a. Artificial Intelligence (AI) and Monte Carlo Simulation-Based Modeling for Predicting Groundwater Pollution Indices and Nitrate-Linked Health Risks in Coastal Areas Facing Agricultural Intensification. Hydrology 13, 59. https://doi.org/10.3390/hydrology13020059

Sanad, H., Moussadek, R., Spaccini, R., Paradiso, R., Oueld Lhaj, M., Zouahri, A., Dakak, H., Mouhir, L., 2026b. Trace metal accumulation in horticulture production systems (HPS) of Mediterranean agro-ecosystems: origins, impacts on soil health, water resources, and plant uptake with sustainable mitigation strategies. Frontiers in Sustainable Food Systems 10. https://doi.org/10.3389/fsufs.2026.1803164

Sanad, H., Moussadek, R., Zouahri, A., Lhaj, M.O., Mouhir, L., Dakak, H., 2025b. Machine learning-integrated hydrogeochemical and spatial modeling of groundwater quality indices for seawater intrusion and irrigation sustainability in coastal agroecosystems of Skhirat Region, Morocco. Journal of Hydrology: Regional Studies 62, 102848. https://doi.org/10.1016/j.ejrh.2025.102848

Sanad, H., Moussadek, R., Zouahri, A., Oueld Lhaj, M., Dakak, H., Manhou, K., Mouhir, L., 2026c. Heavy Metal-Induced Variability in Leaf Nutrient Uptake and Photosynthetic Traits of Avocado (Persea americana) in Mediterranean Soils: A Multivariate and Probabilistic Modeling of Soil-to-Plant Transfer Risks. Plants 15. https://doi.org/10.3390/plants15020205

Sanad, H., Oueld lhaj, M., Zouahri, A., Saafadi, L., Dakak, H., Mouhir, L., 2024d. Groundwater pollution by nitrate and salinization in Morocco: a comprehensive review. Journal of Water and Health 22, 1756–1773. https://doi.org/10.2166/wh.2024.024

Saraswat, A., Ram, S., AbdelRahman, M.A., Raza, M.B., Golui, D., Hc, H., Lawate, P., Sharma, S., Dash, A.K., Scopa, A., 2023. Combining fuzzy, multicriteria and mapping techniques to assess soil

fertility for agricultural development: A case study of Firozabad District, Uttar Pradesh, India. Land 12, 860.

Shokr, M.S., Jalhoum, M.E., Sayed, A.S., Saeed, M., Rebouh, N.Y., Mohamed, E.S., Yousif, I.A., Abdelhameed, H.H., 2025. Assessment of soil quality in arid zones using principal component analysis and GIS-based modeling. PLoS One 20, e0337063.

Shokri, N., Robinson, D.A., Afshar, M., Alewell, C., Aminzadeh, M., Arthur, E., Broothaerts, N., Campbell, G.A., Eklund, L., Gupta, S., 2025. Rethinking global soil degradation: Drivers, impacts, and solutions. Reviews of geophysics 63, e2025RG000883.

Wang, J., Yang, X., Huang, S., Wu, L., Cai, Z., Xu, M., 2025. Long-term combined application of organic and inorganic fertilizers increases crop yield sustainability by improving soil fertility in maize–wheat cropping systems. Journal of Integrative Agriculture 24, 290–305. https://doi.org/10.1016/j.jia.2024.07.003

Wang, L., He, Z., Zhao, W., Wang, C., Ma, D., 2022. Fine Soil Texture Is Conducive to Crop Productivity and Nitrogen Retention in Irrigated Cropland in a Desert-Oasis Ecotone, Northwest China. Agronomy 12. https://doi.org/10.3390/agronomy12071509

Wang, Y.Q., Shao, M.A., 2013. SPATIAL VARIABILITY OF SOIL PHYSICAL PROPERTIES IN A REGION OF THE LOESS PLATEAU OF PR CHINA SUBJECT TO WIND AND WATER EROSION. Land Degradation & Development 24, 296–304. https://doi.org/10.1002/ldr.1128

Wang, Z., Wang, S., Xu, L., Guo, Q., Chen, Y., Qiu, W., Sun, J., 2025. Comparative Evaluation Methods of Comprehensive Soil Fertility in Jiangsu's Coastal Saline–Alkali Land. Land 14. https://doi.org/10.3390/land14030469

Xie, X., Cai, J., Yang, X., Qiu, H., Liu, Y., Zhang, Y., 2024. Integrated assessment of soil quality and contaminant risks in salinized farmland adjacent to an oil-exploitation zone: insights from the Yellow River Delta. Scientific Reports 14, 29369.